Pergamon

Polyhedron Vol. 14, No. 17–18, pp. 2429–2439, 1995

0277–5387/95 $9.50+0.00

0277–5387(95)00069–0

TETRAARYL-METHANE ANALOGUES IN GROUP 14—4.† $Ph_{4-n}M(p\text{-Tol})_n$ ($n = 0$–4, M = Si, Ge, Sn, Pb). SYNTHESIS, STRUCTURAL AND SPECTROSCOPIC DATA, AND SEMI-EMPIRICAL CALCULATIONS: MUTUAL INTERACTION OF TETRAHEDRAL σ-ORBITALS (SYMMETRY AND ELECTRONEGATIVITY) AND DELOCALIZED σ^*-LUMOS (π-LEWIS ACIDITY)

MICHAEL CHARISSÉ, BERND MATHIASCH and MARTIN DRÄGER‡

Institut für Anorganische Chemie und Analytische Chemie der Johannes Gutenberg-Universität, D-55099 Mainz, Germany

and

UMBERTO RUSSO‡

Istituto di Chimica Inorganica, Metallorganica ed Analitica di Università degli Studi di Padova, Via Loredan 4, I-35131 Padova, Italy

(*Received* 25 *November* 1994; *accepted* 18 *January* 1995)

Abstract—The 20 compounds mentioned in the title have been synthesized by lithium (M = Si) or Grignard methods (M = Ge, Sn, Pb). The crystal structure of $Ph_3Sn(p\text{-Tol})$, a survey of the 10 known structures and spectroscopic data (NMR, Mössbauer, IR, Raman) are given. A change of the symmetry of the formally tetrahedral MC_4 backbone arises if M = Si and Ge (elongation along one S_4 or C_3 axis) are altered to M = Sn and Pb (contraction along one S_4 axis). The order of $\delta(^{13}C\text{-}ipso)$ points to a decrease in the electronegativities along Pb ≫ Sn > Ge > Si. The ^{29}Si, ^{119}Sn and ^{207}Pb NMR chemical shifts exhibit a "sagging" along each series, which is described analytically in terms of a quadratic equation. The linear part of this equation is interpreted as an inductive contribution which changes its sign if M is changed from silicon to tin and lead. The quadratic part reflects the different population of a low-lying LUMO with charge given by the aromatic groups. This LUMO is slightly antibonding in the case of silicon and slightly bonding for tin and lead. The "π-acceptor" properties of M explain the upfield NMR shifts $^{29}Si/^{119}Sn/^{207}Pb$ of $MAryl_4$ compounds in comparison with $MAlkyl_4$.

On the basis of experimental data obtained from closely related series of compounds, the group 14 NMR chemical shifts can be discussed in terms of two main effects, the polarity of the group 14 σ-bonds and a charge flow into the related σ^*-LUMOs.[2,3] On condition that in such a series of compounds the polarity contribution of the substituents and the charge flow situation remain constant, electronegativity values (ENs) for the group 14 elements can be derived from NMR chemical shifts. Two unambiguous results are: EN(Ge) > EN(Si)[4] and EN(Pb) ≫ EN(Ge, Sn).[2] These results are in accordance with the "thermochemical" Pauling electronegativity scale.[5a] For group 15, electronegativities have been derived in the same manner (*cf.* ref. 6).

In order to gain additional support for the chemical shift-based group 14 electronegativity scale, the

†Part 3: ref. 1.

‡Authors to whom correspondence should be addressed.

series of compounds $Ph_{4-n}M(p\text{-Tol})_n$ ($n = 0$–4, M = Si, Ge, Sn, Pb) has been synthesized and investigated. Some results for the compounds with M = Si and Sn were given previously.[7]

In addition to the results concerning the occupied group 14 orbitals, the spectroscopic data of the synthesized series of compounds provide indications of the π-Lewis acidity of the group 14 σ^*-LUMOs. In order to gain an impression of the energetic position of the LUMOs, semi-empirical calculations have been performed.

RESULTS

Syntheses of $Ph_{4-n}M(p\text{-Tol})_n$ (n = 0–4; M = Si, Ge, Sn, Pb)

The mixed germanium and lead compounds have been synthesized via Grignard reactions. Migrations of the substituents (as discussed in ref. 8) did not occur. The syntheses of $Ph_{4-n}M(p\text{-Tol})_n$ (M = Si, Sn) have been described previously.[7]

Molecular structure of $Ph_3Sn(p\text{-Tol})$

The overall C_1 symmetric molecule $Ph_3Sn(p\text{-Tol})$ (Fig. 1, Table 1) crystallizes in the orthorhombic space group *Pbca*. Table 2 gives a survey of the bond and torsion angles of the hitherto described structures of molecules of the type $Ph_{4-n}M(p\text{-Tol})_n$. All the compounds listed in Table 2 undergo a distortion along one of the three S_4 axes of the "ideally" tetrahedral geometry, except $Si(p\text{-Tol})_4$ and $Ge(p\text{-Tol})_4$. These two compounds are distorted along one of the four C_3 axes of the "ideally" tetrahedral geometry (three angles less and three angles greater than the tetrahedral value). In the other silicon and germanium compounds, the formal tetrahedron is elongated along its unique S_4 axis, which is perfect for the homogeneous compounds and approximate for the mixed compounds. The elongation results in two angles less and four angles greater than the tetrahedral value. For the tin and lead derivatives, the tetrahedron is contracted along its S_4 axis (two angles greater and four angles less than the tetrahedral value).

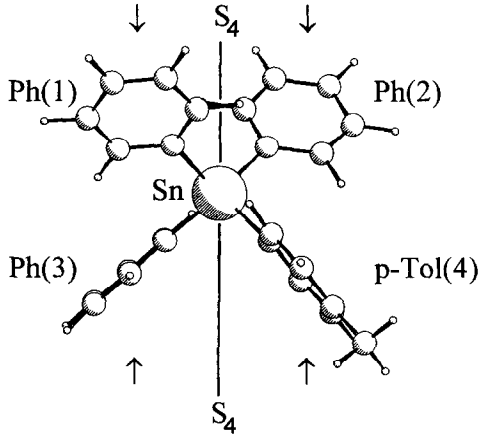

Fig. 1. The $Ph_3Sn(p\text{-Tol})$ molecule. The molecule is compressed along the outlined S_4 axis.

Table 2 shows three general trends. Firstly, for Ph_4M, the bond angle 1 is less and the bond angle 2 is larger than for $M(p\text{-Tol})_4$ (except for M = Ge). Secondly, in both of the series $Ph_{4-n}M(p\text{-Tol})_n$ (M = Si, Sn), the bond angles do not depend linearly upon n. Thirdly, the bond angle 1 increases and the bond angle 2 decreases in the order Si > Ge > Sn > Pb.

An analysis of the data by logarithmical regression showed that this increase of bond angle 1 is parabolically correlated with the increase of the M—C bond length. For Ph_4C, with the smallest M—C bond length of 1.553 Å, angle 1 is 106.7°, and for $Pb(p\text{-Tol})_4$, with the greatest M—C bond length of 2.217 Å, this angle is 115.4°. The point of inversion, i.e. the ideal tetrahedral value of 109.5°, is at a bond length of 2.0 Å. The tetrahedron in compounds with a bond length M—C smaller than this value (M = C, Si, Ge) is always elongated and the tetrahedron in compounds with d(M—C) > 2.0 Å (M = Sn, Pb) is always contracted.

^{13}C *NMR chemical shifts*

Table 3 shows the ^{13}C NMR chemical shift data for the phenyl and *p*-tolyl groups in $CDCl_3$. Contrary to the non-linear behaviour of the NMR data of the central atoms, the ^{13}C NMR chemical shifts show a strongly linear dependence on the number of *p*-tolyl groups n. The increments when changing one phenyl group into a *p*-tolyl group are within the range ±0 to ±0.3 ppm and have the highest value for the ^{13}C-*ipso* atoms (increments in ppm for ^{13}C-*ipso* Ph/*p*-Tol: Si, 0.26/0.26; Ge, 0.20/0.23; Sn, 0.20/0.16; Pb, 0.10/0.07). The chemical shifts of the methyl-^{13}C atoms are not affected by the different nature of the central atom or a different number of *p*-tolyl groups, and vary statistically at a value of 21.4 ± 0.1 ppm.

^{13}C *NMR coupling to* ^{29}Si, ^{119}Sn *and* ^{207}Pb

The averages of the ^nJ values [$(\Sigma(^nJ)/4$; full tables of the coupling constants $^nJ(^{13}C\text{–}^xM)$, the calculated[18] reduced coupling constants ^1K and the average values $(\Sigma^1K)/4$ in $CDCl_3$ are deposited as supplementary material with the Editor, from whom copies are available on request] are nearly

Table 1. Bond lengths and angles for the $Ph_3Sn(p\text{-Tol})$ molecule

Bond lengths (Å)		Torsion angles (°)	
Sn—C(11)	2.135(8)	Four small angles (angle 1)	
Sn—C(21)	2.125(8)	C(21)—Sn—C(31)—C(32)	+0.5(6)
Sn—C(31)	2.122(8)	C(31)—Sn—C(11)—C(12)	−1.5(6)
Sn—C(41)	2.116(8)	C(11)—Sn—C(41)—C(42)	−4.6(7)
		C(41)—Sn—C(21)—C(22)	−6.8(6)
Sn—C (average)	2.125		
$C—C_{arom}$ (average)	1.365	Four medium angles (angle 2)	
C(44)—Me(4)	1.506(13)	C(11)—Sn—C(21)—C(22)	−53.3(7)
		C(31)—Sn—C(41)—C(42)	−57.8(7)
		C(11)—Sn—C(31)—C(32)	−58.7(7)
Bond angles (°)		C(21)—Sn—C(11)—C(12)	−58.7(7)
Two angles widened (angle 1)			
C(31)—Sn—C(41)	110.7(3)	Four high angles (angle 3)	
C(11)—Sn—C(21)	111.1(3)	C(41)—Sn—C(31)—C(32)	+59.7(7)
		C(41)—Sn—C(11)—C(12)	+61.8(7)
		C(21)—Sn—C(41)—C(42)	+63.1(7)
		C(31)—Sn—C(21)—C(22)	+65.2(7)
Four angles compressed (angle 2)			
C(11)—Sn—C(31)	107.4(3)		
C(11)—Sn—C(41)	108.6(3)		
C(21)—Sn—C(41)	109.5(3)		
C(21)—Sn—C(31)	109.6(3)		

constant along each series and are, on that basis, independent of the substitution of phenyl by *p*-tolyl groups.

^{29}Si, ^{119}Sn *and* ^{207}Pb *NMR data*

By plotting the NMR chemical shifts of ^{29}Si,[7] ^{119}Sn[7] and ^{207}Pb (Fig. 2, Table 4) versus the number of *p*-tolyl groups in the series $Ph_{4-n}M(p\text{-Tol})_n$ (M = Si, Sn, Pb; n = 0–4), a "sagging" is observed that can be fitted by numerical equations:

$$\delta(n) = (n-2)^2 * a + (n-2) * b + c \qquad n = 0, 1, \ldots, 4. \quad (1)$$

Mössbauer parameters

The Mössbauer parameters in Table 5 have been obtained for Ph_4Sn and the three series $Ph_{4-n}Sn(o\text{-Tol})_n$, $Ph_{4-n}Sn(m\text{-Tol})_n$ and $Ph_{4-n}Sn(p\text{-Tol})_n$ (n = 1–4) under the same respective conditions for the 13 compounds.

The isomeric shifts exhibit no systematic order and vary insignificantly from 1.35 to 1.39. The trends Ph_4Sn versus $Sn(o\text{-Tol})_4$ and $Sn(m\text{-Tol})_4$ parallel those from the literature;[19] the trend versus $Sn(p\text{-Tol})_4$ is reversed. The overall sensitivity of the Mössbauer isomeric shift is too low for the definite inductive changes $\Delta\delta/4$ of the NMR chemical shifts in Table 4 to be mirrored.

No quadrupole splitting was found for the heterogeneous compounds. Firstly, with regard to the geometry, the perfect S_4 symmetry of the homogeneous compounds remains nearly perfect for the heterogeneous compounds (Table 2). Secondly, with regard to the electronic imbalance of the additional methyl group, the sensitivity of the Mössbauer quadrupole splitting is too low to mirror the definite excess populations of the LUMOs in terms of the NMR chemical shifts (Table 4, Fig. 2).

The only data with significant variations are those for the peak area *A*. Obviously, different Debye temperatures for the different members of each compound series exist. Unfortunately, all available crystal structure determinations were undertaken at room temperature and a direct comparison with the determined equivalent isotropic displacements of tin is not possible. Further, no direct connection to the vibrational data could be recognized.

Vibrational data

IR and Raman data of $Ph_{4-n}Si(p\text{-Tol})_n$, $Ph_{4-n}Ge(p\text{-Tol})_n$, $Ph_{4-n}Sn(p\text{-Tol})_n$ and $Ph_{4-n}Pb(p\text{-Tol})_n$

Table 2. Survey of the known geometric data concerning the S_4 symmetry of the MC_4 backbone in phenyl/*p*-tolyl-substituted compounds $Ph_{4-n}M(p\text{-Tol})_n$ (M = Si, Ge, Sn, Pb)

Compound	Space group, molecular symmetry[a]	d(M—C) (Å)	Related bond angles (°)		Related torsion angles (°)		
			Angle 1	Angle 2	Angle 1	Angle 2	Angle 3
Ph_4C[9]	$P\bar{4}2_1c$, S_4-e	1.553(3)	106.7(2)	110.9(2)	11.1[b]	48.1[b]	72.7[b]
Ph_4Si[10]	$P\bar{4}2_1c$, S_4-e	1.877(2)	108.1(1)	110.1(1)	7.6[b]	52.0[b]	68.3[b]
$Ph_3Si(p\text{-Tol})$[7]	*Pbca*, S_4-e	1.875(7)[b]	107.9(4)[c]	110.3(5)[c]	7.7(34)[c]	51.8(3)[c]	68.7(3)[c]
$Si(p\text{-Tol})_4$[11]	*Pc*, C_3-e	1.873(5)[b]	108.3(1)[c]	110.1(5)[c]	[d]	[d]	[d]
Ph_4Ge[12,13]	$P\bar{4}2_1c$, S_4-e	1.956(1)	108.8(2)	109.8(2)	5.3(2)[b]	54.4(2)[b]	65.8(2)[b]
$Ph_3Ge(p\text{-Tol})$[e]	*Pbca*						
$Ge(p\text{-Tol})_4$[11]	*Pc*, C_3-e	1.948(8)[b]	108.1(8)[c]	110.2(6)[c]	[d]	[d]	[d]
Ph_4Sn[14]	$P\bar{4}2_1c$, S_4-c	2.139(4)	111.2(2)	108.6(1)	3.1[b]	57.4[b]	62.1[b]
$Ph_3Sn(p\text{-Tol})$	*Pbca*, S_4-c	2.125(8)[b]	110.9(3)[c]	108.8(10)[c]	3.4(29)[c]	57.4(28)[c]	62.2(27)[c]
$Sn(p\text{-Tol})_4$[15]	$I\bar{4}$, S_4-c	2.147(6)	114.4(3)	107.0(2)	13.2[b]	49.1[b]	69.3[b]
Ph_4Pb[1,16]	$P\bar{4}2_1c$, S_4-c	2.202(9)	111.6(5)[16]	108.6(1)[16]	1.8[1]	58.9[1]	60.5[1]
$Pb(p\text{-Tol})_4$[17]	$I\bar{4}$, S_4-c	2.217(6)	115.4(3)	106.6(1)	13.9(3)	48.0(3)	70.1(3)

[a] Perfect or approximate point symmetry: *e*, elongated along "S_4" or "C_3"; *c*, contracted along "S_4".
[b] Calculated from the data given in the literature.
[c] Average values.
[d] No regularity of torsion angles (12 different values).
[e] Isostructural with $Ph_3Si/Sn(p\text{-Tol})$, always twinned crystals.

Table 3. ^{13}C NMR chemical shift data in $CDCl_3$ for the series $Ph_{4-n}M(p\text{-Tol})_n$ (n = 0–4, M = Si, Ge, Sn, Pb) (ppm)

	Phenyl				*p*-Tolyl				
	C(1)	C(2,6)	C(3,5)	C(4)	C(1)	C(2,6)	C(3,5)	C(4)	C(Me)
Ph_4Si	134.3	136.5	127.9	129.6					
$Ph_3Si(p\text{-Tol})$	134.5	136.4	127.8	129.5	130.5	136.4	128.8	139.6	21.4
$Ph_2Si(p\text{-Tol})_2$	134.8	136.5	127.8	129.4	130.8	136.4	128.7	139.5	21.5
$PhSi(p\text{-Tol})_3$	135.1	136.5	127.8	129.4	131.1	136.5	128.7	139.4	21.5
$Si(p\text{-Tol})_4$					131.3	136.4	128.7	139.3	21.5
Ph_4Ge	136.2	135.4	128.3	129.1					
$Ph_3Ge(p\text{-Tol})$	136.4	135.4	128.3	129.1	132.4	135.4	129.1	139.0	21.4
$Ph_2Ge(p\text{-Tol})_2$	136.6	135.4	128.2	129.1	132.6	135.4	129.1	138.9	21.4
$PhGe(p\text{-Tol})_3$	136.7	135.4	128.2	129.1	132.8	134.2	129.4	138.8	21.5
$Ge(p\text{-Tol})_4$					133.1	135.4	129.0	138.7	21.4
Ph_4Sn	138.0	137.3	128.6	129.1					
$Ph_3Sn(p\text{-Tol})$	138.2	137.3	128.6	129.1	134.0	137.3	129.6	139.0	21.4
$Ph_2Sn(p\text{-Tol})_2$	138.4	137.2	128.6	129.0	134.2	137.2	129.5	138.9	21.4
$PhSn(p\text{-Tol})_3$	138.6	137.2	128.6	129.0	134.4	137.2	129.5	138.9	21.4
$Sn(p\text{-Tol})_4$					134.5	137.2	129.4	138.8	21.5
Ph_4Pb	150.1	137.7	129.5	128.6					
$Ph_3Pb(p\text{-Tol})$	150.3	137.6	129.4	128.5	146.2	137.6	130.3	138.4	21.3
$Ph_2Pb(p\text{-Tol})_2$	150.3	137.6	129.4	128.4	146.3	137.5	130.3	138.3	21.3
$PhPb(p\text{-Tol})_3$	150.4	137.6	129.4	128.5	146.4	137.5	130.3	138.3	21.3
$Pb(p\text{-Tol})_4$					146.4	137.4	130.1	138.1	21.3

(n = 0–4) were collected (1100–200 cm^{-1} for IR and 1100–50 cm^{-1} for Raman: full tables are deposited as supplementary material with the Editor, from whom copies are available on request).

Previous work on mono- and disubstituted derivatives of benzene and specifical on group 14 phenyl compounds[21] provided enough information to obtain assignments for nearly all the peaks observed. The assignments are limited by degeneration of certain modes, splitting of the ring modes (caused by multiple aryl substitution on the same central atom) and mixing of ring and skeletal modes below 300 cm^{-1}. The nomenclature for phenyl derivatives[22] and for *p*-tolyl derivatives[23] was followed.

The stretching vibration ν_7 of *p*-tolyl occurs only a few wavenumbers below q of phenyl. In all cases a small decrease from Ph_4M to $M(p\text{-Tol})_4$ is found: Si, 1113–1107 cm^{-1}; Ge, 1088–1087 cm^{-1}; Sn, 1076–1070 cm^{-1}; Pb, 1062–1060 cm^{-1}. In no case was a splitting of both vibrations observed.

†Both tetrahedra of the described S_4 symmetric molecules $Ge(C_6F_5)_4$ and $Sn(C_6F_5)_4$ are elongated along the S_4 axis, the bond angles C—M—C (2x/4x) are 105.4°/111.5° and 105.0°/111.7°, the bond lengths are Ge—C 1.957(4) Å and Sn—C 2.126(8) Å.

DISCUSSION

Symmetry

The π–π interactions between aromatic groups occur as the sum of π-electron repulsions and attractive interactions between the π-system and the σ-framework.[24] In the series of compounds of Table 2, these interactions depend on the bond distance M–Aryl. At a hypothetical bond distance d(M—C) of 2.0 Å (see Results), attraction and repulsion between the phenyl and *p*-tolyl groups are well balanced, so that an ideal tetrahedral geometry would be realized. In compounds with d(M—C) < 2.0 Å (M = C, Si, Ge), the increased repulsion is outweighed by an elongated tetrahedron; for d(M—C) > 2.0 Å (M = Sn, Pb), the increased attractive interactions are compensated by a compression of the tetrahedron. For a discussion on the influence of an even greater repulsion, see ref. 25.†

These changes of the C—M—C bond angles, altering the inductive influence of the substituents on the central atom through the σ-bonding orbitals, can be noticed in the ^{29}Si, ^{119}Sn and ^{207}Pb NMR spectroscopic data. The linear term "$(n-2)*b$" (see Results) mirrors the extent and direction of the tetrahedral distortion by a negative coefficient "b" in the case of elongation (Si) and a positive coefficient "b" in the case of compression (Sn, Pb).

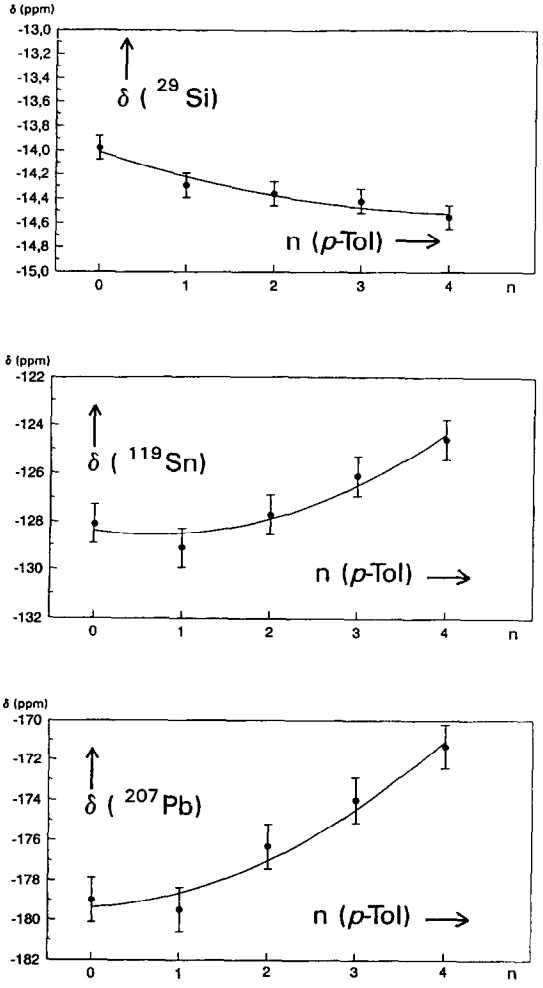

Fig. 2. ^{29}Si, ^{119}Sn and ^{207}Pb NMR chemical shifts of $Ph_{4-n}M(p\text{-Tol})_n$ versus n with quadratic fits.

Electronegativities

Figure 3 illustrates the development of the phenyl and *p*-tolyl ^{13}C-*ipso* NMR chemical shifts for the four series of compounds. It gives a clear sequence of increasing electronegativity in the order

Table 5. Mössbauer effect parameters at 80.0 K (δ, isomeric shift; Γ, half-width value; A, peak area)

Compound	δ^a (mm s^{-1})	Γ (mm s^{-1})	A (mm s^{-1})
Ph_4Sn	1.38	0.90	0.088
$Ph_3Sn(o\text{-Tol})$	1.38	0.87	0.052
$Ph_2Sn(o\text{-Tol})_2$	1.38	0.87	0.064
$PhSn(o\text{-Tol})_3$	1.38	0.90	0.076
$Sn(o\text{-Tol})_4$	1.39	0.91	0.057
$Ph_3Sn(m\text{-Tol})$	1.37	0.87	0.056
$Ph_2Sn(m\text{-Tol})_2$	1.37	0.89	0.051
$PhSn(m\text{-Tol})_3$	1.36	0.86	0.056
$Sn(m\text{-Tol})_4$	1.37	0.87	0.056
$Ph_3Sn(p\text{-Tol})$	1.39	0.94	0.103
$Ph_2Sn(p\text{-Tol})_2$	1.35	0.92	0.084
$PhSn(p\text{-Tol})_3$	1.35	0.96	0.105
$Sn(p\text{-Tol})_4$	1.37	0.96	0.076

[a] Relative to room temperature SnO_2. Reference data from the literature[19] (converted from $CaSnO_3$ into SnO_2 reference by adding 0.1 mm s^{-1}):[20] Ph_4Sn, 1.36; $Sn(o\text{-Tol})_4$, 1.37; $Sn(m\text{-Tol})_4$, 1.35; $Sn(p\text{-Tol})_4$, 1.38 mm s^{-1}.

Si < Ge < Sn ≪ Pb in terms of a reduction of the shielding of the ^{13}C-*ipso* atoms. The thermochemical EN values of Pauling are in the order: C, 2.55; Si, 1.90; Ge, 2.01; Sn, 1.96; Pb, 2.33.[5a]

^{29}Si, ^{119}Sn and ^{207}Pb NMR: inductive contribution

In the equations used for the fit of the observed "sagging" (see Results), the constant term "c" is an indicator of the different sensitivities of the ^{29}Si, ^{119}Sn and ^{207}Pb NMR chemical shift scales. The linear term "$(n\text{-}2) * b$" represents the difference between the inductive influence of the phenyl and *p*-tolyl groups. It reflects the shifting of charge between the respective aromatic groups and the

Table 4. NMR chemical shifts [δ^{29}Si, δ^{119}Sn and δ^{207}Pb in $CDCl_3$ (ppm)], "inductive correction"[a] $\Delta\delta/4$ and "$[\delta(Ph_4M)+n\times(\Delta\delta/4)]-\delta$"[b] (in parentheses)

M	Ph_4M	$Ph_3M(p\text{-Tol})$	$Ph_2M(p\text{-Tol})_2$	$PhM(p\text{-Tol})_3$	$M(p\text{-Tol})_4$	$\Delta\delta/4$
Si	−13.98	−14.29	−14.36	−14.42	−14.55	−0.1425
		(0.168)	(0.095)	(0.013)		
Sn	−128.1	−129.1	−127.7	−126.1	−124.6	+0.875
		(1.88)	(1.4)	(0.63)		
Pb	−179.0	−179.5	−176.3	−174.0	−171.3	+1.925
		(2.43)	(1.15)	(0.78)		

[a] Sum of inductive contribution and "difference of the basic populations of the LUMOs".
[b] Excess population of the LUMOs (Fig. 4).

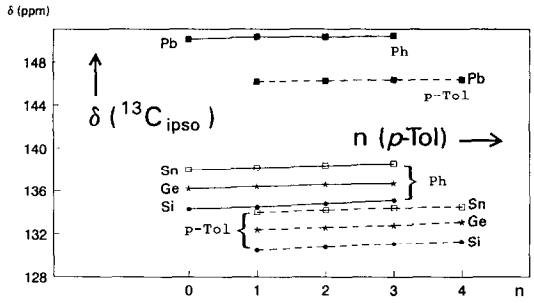

Fig. 3. ^{13}C-*ipso* NMR chemical shifts for the four series $Ph_{4-n}M(p\text{-Tol})_n$ (M = Si, Ge, Sn, Pb and n = 0–4). Phenyl signals: full lines; *p*-tolyl signals: broken lines.

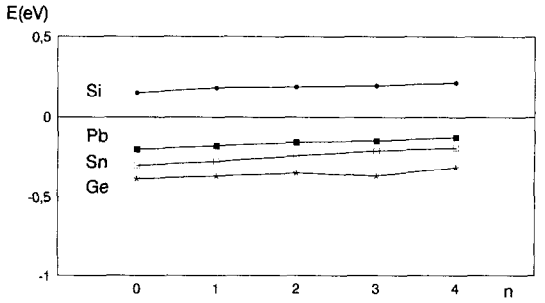

Fig. 4. Semi-empirical calculated LUMO energies of $Ph_{4-n}M(p\text{-Tol})_n$ versus n.†

central atom along the bonding σ-orbitals. The contribution per group is $\Delta\delta/4$ [$\Delta\delta = \delta(Ph_4M) - \delta(M(p\text{-Tol})_4)$; *cf.* Table 4]. The difference $\Delta\delta$ is negative for M = Si and positive for M = Sn and Pb, and corresponds to the change of symmetry of the MC_4 backbone (see above). This parallelism confirms the assumption that the bonding σ-orbitals achieve the main control of $\Delta\delta$. Only a minor contribution arises from the difference of the basic population of the LUMOs (see below).

^{29}Si, ^{119}Sn *and* ^{207}Pb *NMR: π-Lewis acidity*

The quadratic term "$(n\text{-}2)^2 * a$" represents a charge flow between the aromatic groups. The flow is possible via the formally unoccupied σ*-orbitals (LUMOs) of the group 14 elements, "π-Lewis acidity" by population with charge from the aromatic groups. To demonstrate the validity of such a model, a semi-empirical calculation of the molecular orbital energies of the 20 compounds was performed (Fig. 4, Table 6). In the case of M = Si, the LUMO is slightly antibonding. For M = Ge, Sn and Pb, the LUMO is within the bonding region, and a population with charge has a stabilizing effect.† Figure 5 shows the excess population of the LUMOs with charge in $Ph_3M(p\text{-Tol})$, $Ph_2M(p\text{-Tol})_2$ and $PhM(p\text{-Tol})_3$ for M = Si, Sn and Pb in addition to the basic population in Ph_4M.

NMR high-field shifts of aromatic-substituted group 14 elements

All NMR signals of the central atom M in $MAryl_4$ compounds are shifted considerably upfield in comparison with the related signals of the $MAlkyl_4$ compounds (Table 7). The only exception is the ^{13}C NMR chemical shift of the compound Ph_4C:[26] carbon four times in a short distance to the deshielding "side-on" position of the aromatic ring current. In the literature,[27–31] the upfield shifts of M in $MAryl_4$ are not explained.

The above-considered π-Lewis acidity of M results necessarily in the upfield shifts seen in Table 7. Two demands are necessary to populate the LUMO of M: firstly, a low energy of this LUMO and, secondly, the presence of a "moveable" charge in the substituent. The positions of the LUMOs of the compounds of Table 7 have been obtained from semi-empirical calculations. Their relative orders are visualized in Fig. 6. Except for M = Pb, the charge donating power of the aromatic substituents is enhanced by the lower LUMO of the $MAryl_4$ compounds. The methyl substituent has a stronger charge-donating capability (the so-called "hyperconjugation")[32] than the ethyl substituent. Accordingly, the MEt_4 signals are always shifted downfield, despite the lower position of the LUMOs of MEt_4.

EXPERIMENTAL

Syntheses

Table 8 gives an overview of the Grignard reactions for the mixed germanium and lead compounds. For the syntheses of the homogeneous compounds MAr_4 see refs 34–37 for silicon, germanium, tin and lead, respectively.

X-ray structure determination

Table 9 contains crystallographic data and structure determination details. Crystals of $Ph_3Sn(p\text{-Tol})$ were obtained by very slow evaporation of a $CHCl_3$ solution. Only crystals of small size had adequate quality for structure determination. The

†The unexpected fact that the calculated LUMO energies for the germanium compounds are lower than the corresponding silicon, tin and lead energies may be the consequence of the incorrectly predicted ground state of the germanium atom by the PM3 method to be $4s^14p^3$ and not $4s^24p^2$.[5b,43]

Table 6. Semi-empirically calculated HOMO and LUMO energies (eV) for the series $Ph_{4-n}M(p\text{-Tol})_n$

		n =				
M		0	1	2	3	4
Si	LUMO	0.15	0.18	0.19	0.20	0.22
	HOMO	−9.45	−9.24	−9.19	−9.18	−9.17
Ge	LUMO	−0.39	−0.37	−0.35	−0.37	−0.32
	HOMO	−9.59	−9.35	−9.31	−9.29	−9.28
Sn	LUMO	−0.30	−0.27	−0.24	−0.21	−0.19
	HOMO	−9.66	−9.46	−9.46	−9.46	−9.45
Pb	LUMO	−0.20	−0.18	−0.16	−0.15	−0.13
	HOMO	−9.59	−9.36	−9.34	−9.31	−9.33

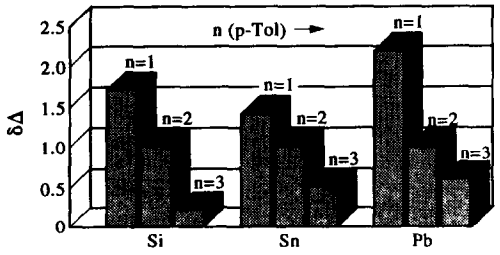

Fig. 5. Excess populations of the LUMOs with charge in $Ph_3M(p\text{-Tol})$, $Ph_2M(p\text{-Tol})_2$ and $PhM(p\text{-Tol})_3$ for M = Si, Sn, Pb in addition to the basic population of Ph_4M in units of relative NMR chemical shifts {scaled on $\delta[Ph_2{}^{29}Si(p\text{-Tol})_2] = 1$ to obtain comparability, values from Table 4}.

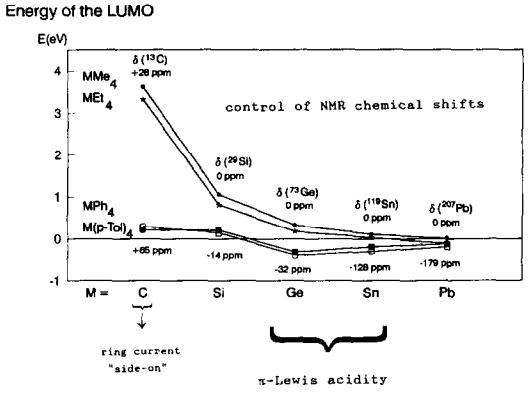

Fig. 6. LUMO energies of $MAlkyl_4$ and $MAryl_4$ compounds.

Table 7. Heteronuclear NMR chemical shifts [δ (ppm)] and semi-empirically calculated LUMO energies (eV)

M		MMe_4	MEt_4	MPh_4	$M(p\text{-Tol})_4$
^{13}C	δ	+28.0[33]	+37.1[33]	+65.0[26]	
	LUMO	+3.63	+3.33	+0.30	+0.22
^{29}Si	δ	0	+8.4[27]	−13.98	−14.55
	LUMO	+1.06	+0.82	+0.15	+0.22
^{73}Ge	δ[28]	0	+17.3	−31.6	
	LUMO	+0.33	+0.18	−0.39	−0.32
^{119}Sn	δ	0	+1.4[27]	−128.1	−124.6
	LUMO	+0.11	+0.03	−0.30	−0.19
^{207}Pb	δ	0	+71.9[31]	−179.0	−171.3
	LUMO	0	−0.11	−0.20	−0.13

experimental density was determined by flotation in an aqueous polytungstate solution. Single crystals were fixed in capillaries for crystallographic investigations by the Weissenberg method and for the collection of the intensity data. Only small amounts of adhesive were used to enable face indexing. The tin atom and all carbon positions were found by direct methods and treated anisotropically. Hydrogen atoms were treated as riding isotropically (joint U values for the aromatic hydrogen atoms and for the three methyl hydrogen atoms, respectively). All calculations were performed at the Zentrum für Datenverarbeitung der Universität Mainz (VAX cluster) with SHELX-76, SHELX-86[42] and local

Table 8. Experimental data for the syntheses of the germanium and lead compounds via Grignard reaction and analytical results

Product	Starting materials	Solvents	Temp.[a] (time, h)	Recryst. from	Yield (%)	M.p. (°C) (lit.)	Elemental analyses[b] Formula (M_r)	C (calc.)	H (calc.)
$Ph_3Ge(p\text{-Tol})$	Ph_3GeBr + *p*-TolMgBr	diethyl ether/ toluene	RT (1) + refl. (16)	petrol. ether–EtOH	30	130–135 (122–123)[38]	$C_{25}H_{22}Ge$ 395.04	76.2 (76.0)	5.6 (5.6)
$Ph_2Ge(p\text{-Tol})_2$	Ph_2GeCl_2 + *p*-TolMgBr	diethyl ether/ toluene	RT (2) + refl. (16)	MeOH	17	98	$C_{26}H_{24}Ge$ 409.07	76.3 (76.3)	5.8 (5.9)
$PhGe(p\text{-Tol})_3$	$BrGe(p\text{-Tol})_3$ + PhMgBr	diethyl ether/ toluene	RT (1) + refl. (16)	MeOH	63	106–107[c]	$C_{27}H_{26}Ge$ 423.09	65.4[c] (76.7)	5.2[c] (6.2)
$Ph_3Pb(p\text{-Tol})$	Ph_3PbI + *p*-TolMgBr	tetrahydrofuran	RT (48) + refl. (3)	EtOH	36	120 (125.5)[40]	$C_{25}H_{22}Pb$ 529.65	56.4 (56.7)	4.1 (4.2)
$Ph_2Pb(p\text{-Tol})_2$	Ph_2PbI_2 + *p*-TolMgBr	diethyl ether	refl. (2)	EtOH	63	115–116 (121–122)[41]	$C_{26}H_{24}Pb$ 543.68	57.2 (57.4)	4.4 (4.5)
$PhPb(p\text{-Tol})_3$	$IPb(p\text{-Tol})_3$ + PhMgBr	diethyl ether	refl. (2)	EtOH	25	183–185	$C_{27}H_{26}Pb$ 557.70	57.4 (58.2)	4.5 (4.7)

[a] RT, room temperature; refl., refluxing solvent.

[b] C and H values were determined in the Institut für Organische Chemie Universität Mainz with a CHN analyser 240 (Perkin–Elmer).

[c] No melting point given in the literature;[38,39] compound contaminated with $Ge_2(p\text{-Tol})_6$.

Table 9. Crystallographic data for $Ph_3Sn(p\text{-Tol})$ and structure determination details

Crystal data (Mo-$K_{\alpha 1}$, $\lambda = 0.70926$ Å)	
Formula, M_r	$C_{25}H_{22}Sn$, 441.09
Crystal habit	hexagonal column
Face indices (distances from a common origin inside the crystal)	1 0 0, −1 0 0 (0.45) mm 0 1 0, 0 −1 0 (0.065) mm 0 0 1, 0 0 −1 (0.065) mm 0 1 −1, 0 −1 1 (0.030) mm
Crystal colour	colourless
Crystal system, space group	orthorhombic, *Pbca* (No. 61)
Unit cell dimensions	$a = 6.644(2)$ Å $b = 17.283(3)$ Å $c = 35.838(7)$ Å
Least squares fit	24 refl., $\theta = 17$–$21°$
Packing: V, Z	4115(1) Å^3, 8
D_{calc}, D_{exp}	1.424, 1.432 g cm^{-3}
Intensity data collection (Mo-K_α, $\lambda = 0.71069$)	
Temperature	24°C
θ range (ω-scan), sin ϑ_{max}/λ	1.5–27.5°, 0.6497 Å^{-1}
Time	6 d
Loss of intensity	none
Independent reflexes	4731
Reflexes used [with $I > 1 * \sigma(I)$]	2380
μ, absorption correction	11.36 cm^{-1}, by face indices
Range of transmission	0.8861–0.8495
Refinement	
Number of variables, refl./var.	239, 9.96
Final R	0.0545
Final R_g	0.0596
Weighting scheme w^{-1}	$\sigma^2(F) + 0.001508 * F^2$
Final difference Fourier maximum	1.2 e Å^{-3} near Sn

programs. Tables of the SHELX input, of final coordinates and thermal parameters, a complete list of bond lengths, bond angles and torsion angles, and a list of F_o/F_c values have been deposited as supplementary material with the Editor, from whom copies may be obtained.

NMR spectroscopy

A Bruker WP/80 DS spectrometer with DEPT pulse sequence at 30°C was used. Frequencies: ^{13}C at 20.15 MHz, ^{29}Si at 15.92 MHz, ^{119}Sn at 29.88 MHz and ^{207}Pb at 16.74 MHz. External standards: $(CH_3)_4Si$, $(CH_3)_4Sn$ and $(CH_3)_4Pb$. Concentration: 100–400 mg of compound/3 cm^3 $CDCl_3$ (Aldrich No. 15, 182-3).

Mössbauer spectroscopy

Mössbauer effect spectra were obtained on a conventional constant-acceleration spectrometer that utilized a room temperature $Ca^{119m}SnO_3$ source and a liquid nitrogen cryostat equipped with a variable temperature insert. Spectra were recorded at 80 K.

IR and Raman spectroscopy

FT-IR were recorded using a Galaxy 2030 spectrometer (Mattson); 4000–200 cm^{-1}, CsI pellets. Raman spectra were recorded using a SPEX 1403 spectrometer; excitation with an He/Ne laser at 633 nm or with a krypton laser at 647 nm; microcrystalline samples in capillaries.

Semi-empirical calculations

All calculations were performed using the MOPAC 6.0 program package on IBM RISC/6000 equipment. The orbital energies have been determined by the use of the PM3 method.[43,44] The molecular geometry was optimized starting from known or closely related crystal structures.

Acknowledgements—We are grateful for financial assistance from the Deutsche Forschungsgemeinschaft, Bonn-Bad Godesberg, Germany, the CNR, Rome, Italy, and the Fonds der Chemischen Industrie, Frankfurt/Main, Germany.

REFERENCES

1. C. Schneider-Koglin, B. Mathiasch and M. Dräger, *J. Organomet. Chem.* 1994, **469**, 25.
2. H.-J. Koglin, K. Behrends and M. Dräger, *Organometallics* 1994, **13**, 2733.
3. U. Kolb, M. Beuter and M. Dräger, *Inorg. Chem.* 1994, **33**, 4522.
4. M. Charissé, M. Mathes, D. Simon and M. Dräger, *J. Organomet. Chem.* 1993, **445**, 39.
5. J. E. Huheey, E. A. Keiter and R. L. Keiter, *Inorganic Chemistry, Principles of Structure and Reactivity*, 4th edn. Harper Collins, New York (1993); (a) pp. 187 and 884; (b) p. 24.
6. E. Bräu, R. Falke, A. Ellner, M. Beuter, U. Kolb and M. Dräger, *Polyhedron* 1994, **13**, 365.
7. M. Charissé, V. Gauthey and M. Dräger, *J. Organomet. Chem.* 1993, **448**, 47.
8. N. Kleiner and M. Dräger, *J. Organomet. Chem.* 1985, **293**, 323.
9. A. Robbins, G. A. Jeffrey, J. P. Chesick, J. Donohue, F. A. Cotton, B. A. Frenz and C. A. Murillo, *Acta Cryst.* 1975, **B31**, 2395.
10. V. Gruhnert, A. Kirfel, G. Will, F. Wallrafen and K. Recker, *Z. Krist.* 1983, **163**, 53.
11. M. Charissé, S. Roller and M. Dräger, *J. Organomet. Chem.* 1992, **427**, 23.
12. P. C. Chieh, *J. Chem. Soc.* (*A*) 1971, 3243.
13. A. Karipides and D. A. Haller, *Acta Cryst.* 1972, **B28**, 2889.
14. V. K. Belsky, A. A. Simonenko, V. O. Reikhsfeld and I. P. Saratov, *J. Organomet. Chem.* 1983, **244**, 125.
15. A. Karipides and K. Wolfe, *Acta Cryst.* 1975, **B31**, 605.
16. V. Busetti, M. Mammi, A. Signor and A. Del Pra, *Inorg. Chim. Acta* 1967, **1**, 424.
17. C. Schneider and M. Dräger, *J. Organomet. Chem.* 1991, **415**, 349.
18. J. A. Pople and D. P. Santry, *Molec. Phys.* 1964, **8**, 1.
19. D. W. Allen, J. S. Brooks and R. Formstone, *J. Organomet. Chem.* 1972, **172**, 299.
20. G. M. Bancroft, *Mössbauer Spectroscopy*, pp. 72 and 241. McGraw-Hill, London (1973).
21. R. D. Kross and V. A. Fassel, *J. Am. Chem. Soc.* 1955, **77**, 5858; E. F. Mooney, *Spectrochim. Acta* 1964, **20**, 1343; D. H. Brown, A. Mohammed and D. W. A. Sharp, *Spectrochim. Acta* 1965, **21**, 659; A. L. Smith, *Spectrochim. Acta* 1968, **24A**, 695; K. M. Mackay, D. B. Sowerby and W. C. Young, *Spectrochim. Acta* 1968, **24A**, 611; J. H. S. Green, *Spectrochim. Acta* 1970, **26A**, 1503; M. E. Bishop, C. D. Schaeffer Jr and J. J. Zuckerman, *Spectrochim. Acta* 1976, **32A**, 1519; M. Dräger and L. Ross, *Z. Anorg. Allg. Chem.* 1980, **207**, 460; F. Höfler, *Monatsh. Chem.* 1976, **107**, 705, 893.
22. D. H. Whiffen, *J. Chem. Soc.* 1956, **47**, 1350.
23. A. Stojiljkovic and D. H. Whiffen, *Spectrochim. Acta* 1958, **12**, 47.
24. C. A. Hunter and J. K. M. Sanders, *J. Am. Chem. Soc.* 1990, **112**, 5525.
25. A. Karipides, C. Forman, R. H. P. Thomas and A. T. Reed, *Inorg. Chem.* 1974, **13**, 811.
26. T. N. Mitchell, *J. Organomet. Chem.* 1983, **255**, 279.
27. R. K. Harris, J. D. Kennedy and W. McFarlane, in *NMR and the Periodic Table* (Edited by R. K. Harris and B. E. Mann), p. 309. Academic Press, London (1978).
28. J. D. Kennedy and W. McFarlane, in *Multinuclear NMR* (Edited by J. Mason), p. 305. Plenum Press, New York (1987).
29. E. A. Williams, in *The Chemistry of Organic Silicon Compounds*, Part 1 (Edited by S. Patai and Z. Rappoport), p. 511. John Wiley, Chichester (1989).
30. B. Wrackmeyer, *Ann. Rep. NMR Spectrosc.* 1985, **16**, 73.
31. B. Wrackmeyer and K. Horchler, *Ann. Rep. NMR Spectrosc.* 1989, **22**, 249.
32. J. March, *Advanced Organic Chemistry*, 4th edn, p. 68. John Wiley, New York (1992).
33. L. P. Lindeman and J. Q. Adams, *Analyt. Chem.* 1971, **43**, 1245.
34. Gmelin, *Handbook of Inorganic and Organometallic Chemistry, Organische Silicium-Verbindungen*, Teil C, 8th edn. Springer, Berlin (1958).
35. Gmelin, *Handbook of Inorganic and Organometallic Chemistry, Organogermanium Compounds*, Part 3, 8th edn. Springer, Berlin (1990).
36. Gmelin, *Handbook of Inorganic and Organometallic Chemistry, Zinnorganische Verbindungen*, Teil 1, 8th edn. Springer, Berlin (1975).
37. Gmelin, *Handbook of Inorganic and Organometallic Chemistry, Organolead Compounds*, Part 3, 8th edn. Springer, Berlin (1992).
38. W. R. Orndorff, D. L. Tabern and L. M. Dennis, *J. Am. Chem. Soc.* 1927, **49**, 2512.
39. R. Schwarz and M. Lewinsohn, *Ber. Dtsch. Chem. Ges.* 1931, **64**, 2352.
40. E. Krause and M. Schmitz, *Ber. Dtsch. Chem. Ges.* 1919, **52**, 2165; F. B. Kipping, *J. Chem. Soc.* 1928, 2365.
41. P. R. Austin, *J. Am. Chem. Soc.* 1932, **54**, 3726.
42. G. Sheldrick, SHELX-76, Program for Crystal Structure Determination, Cambridge, U.K. (1976); SHELX-86, Göttingen (1986).
43. J. J. P. Stewart, *J. Comput. Chem.* 1991, **12**, 320.
44. J. J. P. Stewart, *J. Comput. Chem.* 1989, **10**, 221.